

# Theory of Andreev blockade in a double quantum dot with a superconducting lead

David Pekker, Po Zhang and Sergey M. Frolov

Department of Physics and Astronomy, University of Pittsburgh, Pittsburgh, PA, 15260

## Abstract

A normal metal source reservoir can load two electrons onto a double quantum dot in the spin-triplet configuration. We show that if the drain lead of the dot is a spin-singlet superconductor, these electrons cannot form a Cooper pair and are blockaded on the double dot. We call this phenomenon Andreev blockade because it arises due to suppressed Andreev reflections. We identify transport characteristics unique to Andreev blockade. Most significantly, it occurs for any occupation of the dot adjacent to the superconductor, in contrast with the well-studied Pauli blockade which requires odd occupations. Andreev blockade is lifted if quasiparticles are allowed to enter the superconducting lead, but it should be observable in the hard gap superconductor-semiconductor devices. A recent experiment tests this model and finds support for several predictions made here [1]. Andreev blockade should be considered in the design of topological quantum circuits, hybrid quantum bits and quantum emulators.



Copyright D. Pekker *et al.*

This work is licensed under the Creative Commons

[Attribution 4.0 International License](https://creativecommons.org/licenses/by/4.0/).

Published by the SciPost Foundation.

Received 25-08-2021

Accepted 28-09-2021

Published 22-10-2021

doi:[10.21468/SciPostPhys.11.4.081](https://doi.org/10.21468/SciPostPhys.11.4.081)



Check for updates

## 1 Introduction

Transport blockade phenomena are interruptions of transmission due to interactions of multiple particles. They are a testbed for new physics related to coherence or conservation of charges, spins, photons and phonons [2–7]. The most iconic is the Coulomb blockade [8–12] which occurs when the energy barrier due to charging prevents electrons from tunneling through e.g. a quantum dot. Double quantum dots are known to demonstrate Pauli blockade due to spin-triplet states. This has been thoroughly studied in a large number of platforms, and is commonly used as an initialization and readout mechanism for quantum dot spin-based qubits [13–15]. The realization of single and double quantum dots coupled to superconductors, with induced Andreev bound states [16–18], brings forward the question of whether there can be blockade phenomena specific to Andreev transport?

In this manuscript, we propose a blockade that appears in transport through a double quantum dot with at least one superconducting lead [19]. The gap in the superconductor prevents single-particle transport through the double dot. However, transport can still take place via the process of Andreev reflection in which two electrons from the double dot enter the superconducting lead as a Cooper pair. We find that if the two electrons have been loaded

in a triplet state, Andreev reflection is suppressed [20–25]. Both Pauli blockade and Andreev blockade involve triplet states of two electrons. However, the origin of the former is the Pauli exclusion principle that prevents electrons from passing through a dot already occupied by an electron of the same spin. The origin of Andreev blockade is angular momentum conservation: a pair of electrons must be in a singlet state in order to tunnel into the superconductor as a Cooper pair, hence electrons in a triplet state have the wrong total spin. While Andreev blockade happens at the dot-lead interface, it still requires two dots to manifest because the system needs to be filled into a low-energy (subgap) triplet state, e.g. with one electron on each dot (Fig. 1). We note that the device depicted in Fig. 1 has been realized experimentally and the basic predictions of our model were confirmed [1]. Another related experiment considered a similar setup with blockade due to spin polarization of the double dot states in high magnetic fields [26].

The transport signatures of Andreev blockade are summarized in Fig. 2 (We introduce the model further below and in the supplemental materials in the interest of presenting the phenomena clearly). It is instructive to compare Andreev blockade to the well-studied Pauli blockade for the case of a double dot with normal leads (Fig. 2(a)). First, we observe that due to Coulomb blockade, transport is only allowed through the double dot in the vicinity of charge degeneracy points, which at finite source-drain voltage bias transform into double-triangle structures in the space of the two gate voltages that change the occupations of the two dots,  $V_{g1}$  vs.  $V_{g2}$  (here in the units of charge occupation).

Pauli blockade leads to suppressed conductance at the  $(1,1) \rightarrow (0,2)$  charge degeneracy point, where  $(n,m)$  denote double dot occupations (Fig. 2(a)). Andreev blockade appears at the two  $(1,\text{odd}) \rightarrow (0,\text{even})$  charge degeneracy points (Fig. 2(b)), i.e. twice as often as Pauli blockade. Andreev blockade is only sensitive to the parity of the charging state of  $QD_1$  due to the particle-hole symmetry in the superconductor. As in the case of Pauli blockade, changing the source-drain bias direction changes which charge degeneracy points are blocked (see supplemental materials). In the case of Andreev blockade, switching the bias direction results in the blockade to the two  $(1,\text{odd}) \rightarrow (2,\text{even})$  charge degeneracy points.

A closer comparison reveals that the conductance triangles in Andreev transport (Fig. 2(b)) are approximately twice as large as in normal transport (Fig. 2(a)). At the same time, there is only one conductance triangle at each charge degeneracy point in Andreev transport, but two in normal transport. Furthermore, Fig. 2(c) shows that the breakdown of Andreev blockade at large source-drain bias is different from Pauli blockade: in Andreev blockade the source-drain bias needs only to exceed the superconducting gap of the lead in order for breakdown to occur, while in Pauli blockade the bias must exceed the  $(0,2)$  singlet-triplet energy (not shown) [13].

In order to understand these manifestations of the Andreev blockade, let us first consider

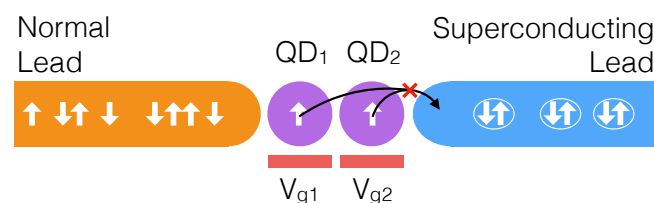


Figure 1: Device schematic: Two quantum dots (labeled  $QD_1$  and  $QD_2$ ) are tunnel coupled to each other and to the two leads. The left, normal metal lead supports only single electron tunneling. The right, superconducting lead supports only Cooper pair tunneling. The chemical potentials on the quantum dots are tuned using two gates (labeled  $V_{g1}$  and  $V_{g2}$ ). Quantum dots are shown in the  $T_+(1, 1)$  configuration, but Andreev blockade also occurs for  $T_0(1, 1)$  and  $T_-(1, 1)$ .

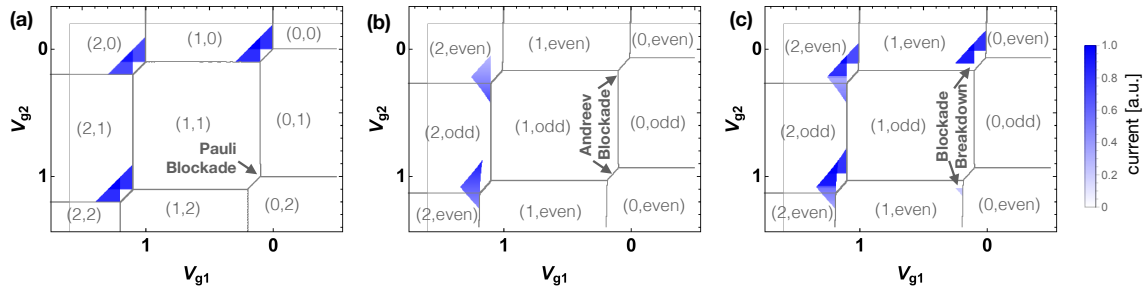


Figure 2: Zero temperature charge stability diagrams comparing Pauli and Andreev blockades. Current through the double quantum dot at fixed source-drain bias voltage is plotted as a function of the gate voltages  $V_{g1}$  and  $V_{g2}$  on the two quantum dots. Gate voltages are in the units of dot charging energies  $U_1 = U_2 = 1$ . Labels in brackets indicate the lowest energy states of the double dot. (a) Pauli blockade: double quantum dot with two normal metal leads at low source-drain bias.  $\Delta_2 = 0$ ,  $\Gamma_2 = 0.01$ , where  $\Delta_2$  is the Andreev coupling in dot 2,  $\Gamma_2$  is the single particle tunneling rate between dot 2 and lead 2. (b) Andreev blockade: double quantum dot with one normal metal lead and one superconducting lead at low source-drain bias.  $\Delta_2 = 0.25$ ,  $\Gamma_2 = 0$ . (c) Breakdown of Andreev blockade: when the source drain bias exceeds the superconducting gap (which we reduce from infinite to  $0.05U_1$  in this plot), the conductance triangles partially reappear.  $\Delta_2 = 0.25$ ,  $\Gamma_2 = 0.01$  if  $|\Delta E| > 0.05$  else 0, where  $\Delta E$  is the energy difference between the initial and final states. Other parameters used: inter-dot charging energy  $U_{12} = 0.1$ , source and drain bias  $V_1 = -V_2 = 0.1$ , tunneling rate between dot 1 and lead 1  $\Gamma_1 = 0.01$ , between dot 1 and dot 2  $\Gamma_{12} = 0.024$ , further details in the supplemental materials.

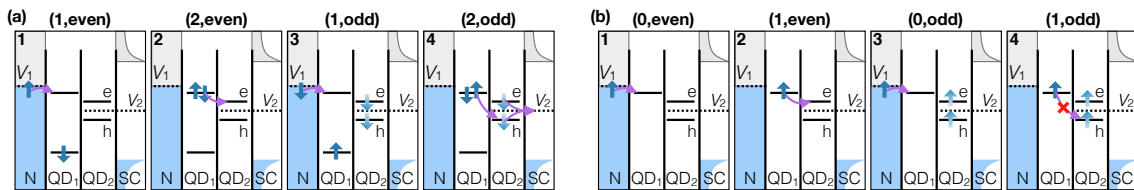


Figure 3: (a) Andreev transport cycle.  $QD_1$  is tuned to the 1-2 charge degeneracy point, while  $QD_2$  is tuned to the vicinity of one of the charge degeneracy points, such that even state is the ground state. The transport cycle consists of four charge states depicted in the Figure. The incoherent electron tunneling processes (which we describe using the master equation formalism) are depicted by purple arrows. Odd parity states of  $QD_2$  are depicted as superpositions of electron and hole states to denote the approximate particle-hole symmetry (i.e. the fact that odd  $\rightarrow$  even transition can occur via either electron addition or electron subtraction). (b) Andreev blockade. Setup identical to panel (a) except the  $QD_1$  is tuned to the 0-1 charge degeneracy point. Andreev blockade occurs in the last step:  $QD_1$  and  $QD_2$  both host a spin-up electron, consequently the spin-up electron on  $QD_1$  cannot tunnel onto  $QD_2$  to make a Cooper pair.

a single quantum dot coupled to a superconducting lead. In the absence of Andreev reflection, the quantum dot can be in one of four states:  $|0\rangle$ ,  $|\uparrow\rangle$ ,  $|\downarrow\rangle$ , or  $|\uparrow\downarrow\rangle$  (corresponding to empty, spin-up electron, spin-down electron, and doubly occupied). Conventionally, the charging state of the dot is denoted as  $\{0, 1, 2\}$  (where the number indicates the number of electrons on the dot). In a quantum dot coupled to a superconductor, Andreev reflection can be functionally understood as a process that hybridizes states in the same parity sector, meaning that in our case it mixes the two even parity states  $|0\rangle$  and  $|\uparrow\downarrow\rangle$ . Therefore, in the presence of Andreev reflection we switch to parity notation  $\{\text{even}, \text{odd}\}$  to denote the state of a quantum dot coupled to a superconducting lead. Starting from an odd parity state we can reach an even parity state by either *adding* or *removing* an electron. Hence, the levels of the quantum dot coupled to a superconducting lead can be thought of as approximately particle-hole symmetric.

The mixing of the empty and doubly occupied states implies that the two charge degeneracy points of the quantum dot nearest to the superconducting lead are equivalent. Therefore, Andreev blockade can only be controlled by the occupancy of the quantum dot nearest to the normal lead, which is the reason why Andreev blockade occurs twice as often as Pauli blockade.

The approximate particle-hole symmetry implies that the conductance is approximately unchanged as the quantum dot nearest to the superconducting lead is tuned from slightly above the charge degeneracy point to slightly below it. That is, conductance can take place on both the particle-like and hole-like side of the charge degeneracy point. On the other hand, the version of the device with two normal metal leads can only support conductance on the particle-like side of the charge degeneracy point. The additional hole-like conductance regime that is present in Andreev transport results in the approximate doubling in the size of conductance triangles in Andreev as compared to normal transport.

The fact there is only one transport triangle at each charge degeneracy point in Andreev transport (Fig.2(b)), while there are two in normal transport (Fig.2(a)), is a consequence of the fact that in Andreev transport two electrons must be moved from the source to the drain lead per transport cycle, while only one electron is moved in normal transport. Normal charge transport cycle goes through three charging states and hence requires a triple charge degeneracy point (i.e. a point at which three charging states become degenerate). The Andreev transport cycle goes through four charging states and hence requires a quadruple charge degeneracy point. In normal transport, finite inter-dot coupling splits the quadruple charge degeneracy point into two triple charge degeneracy points and hence the number of conductance triangles doubles resulting in characteristic hexagonal patterns of charge transport in double quantum dot systems. On the other hand, the number of triangles in Andreev transport remains unchanged as all four charging states are required for transport.

## 2 Andreev charge transport cycle

We use the master equation formalism to describe electron transport (see supplemental materials for details of the method). Our strategy is to begin by considering the eigenstates of  $QD_1$  and of  $QD_2$  independently. We assume weak interdot tunnel coupling so that the double dot states are well approximated by direct products of the eigenstates of the two dots. The charge transport cycle involves sequential incoherent transitions between  $QD_1$  and  $QD_2$  eigenstates.

To describe the quantum states of the double-dot system we use the Hamiltonian

$$H = H_1 + H_2 + U_{12}(n_{1,\uparrow} + n_{1,\downarrow})(n_{2,\uparrow} + n_{2,\downarrow}), \quad (1)$$

where  $U_{12}$  is the inter-dot interaction strength,  $n_{i,\sigma}$  is the electron number operator on dot  $i$ ,

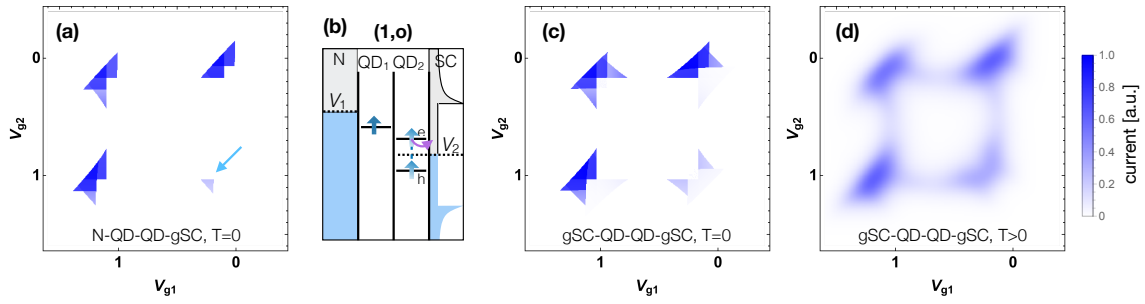


Figure 4: Interplay of Andreev and spin blockade. (a) Charge stability diagram for a N-QD-QD-(gapless SC) system showing a transport pattern consisting of conventional transport features, Andreev transport features, and a new feature indicated by the blue arrow. The new feature is a consequence of tunneling process depicted in (b).  $\Gamma_2 = 0.01$ , other parameters are the same as those in Fig. 2b and 2c. (b) Tunneling process enabled by quasiparticles in the superconducting leads that results in the clearing of the inter-dot triplet. (c) Charge stability diagram for a (gapless SC)-QD-QD-(gapless SC) system.  $\Delta_1 = 0.25$ , other parameters are the same as those in panel (a). (d) Same as (c) but at  $T = 0.05U_1$ .

and  $H_i$  is the single dot Hamiltonian

$$H_i = \sum_{\sigma} \epsilon_{i,\sigma} n_{i,\sigma} + U_i n_{i,\uparrow} n_{i,\downarrow} + \left( \Delta_i c_{i,\uparrow}^{\dagger} c_{i,\downarrow}^{\dagger} + \text{h.c.} \right) + eV_i \sum_{\sigma} (1 - n_{i,\sigma}), \quad (2)$$

where  $\epsilon_{i,\uparrow}$  and  $\epsilon_{i,\downarrow}$  are the single-electron energies,  $U_i$  is the quantum dot charging energy,  $\Delta_i$  is the Andreev reflection amplitude ( $\Delta_i = 0$  for normal metal leads), and the operator  $c_{i,\uparrow}^{\dagger}, c_{i,\downarrow}^{\dagger}$  creates a pair of electrons on the quantum dot, and  $V_i$  is the electrochemical potential of the lead. We use the  $eV_i$  term to account for the energy of an electron as it leaves the quantum dot and enters the adjacent lead. This term is crucial for describing Andreev reflection in which pairs of electrons coherently move between the quantum dot and the proximate superconducting lead [27]. For the quantum dot coupled to the superconducting lead, the eigenstates that play a role in transport are the two odd parity eigenstates ( $|\uparrow\rangle$  and  $|\downarrow\rangle$ ) and the lower energy even parity eigenstate ( $|e\rangle$ ) that is the superposition of the states  $|0\rangle$  and  $|\uparrow\downarrow\rangle$ .<sup>1</sup>

Each Andreev charge transport cycle adds a Cooper pair to the superconducting lead. We first consider a cycle without Andreev blockade (Fig. 3(a)). QD<sub>1</sub> is tuned to the charge 1-2 degeneracy point, with the 1 state being slightly lower in energy, while QD<sub>2</sub> is tuned to the even-odd degeneracy point with the even state being slightly lower in energy. The transport cycle consists of four steps: (1) an electron from the normal lead moves onto QD<sub>1</sub>; (2) an up-spin electron moves from QD<sub>1</sub> to QD<sub>2</sub> resulting in QD<sub>2</sub> being excited into the odd state; (3) another electron from the normal lead moves onto QD<sub>1</sub>; (4) a down-spin electron from QD<sub>1</sub> moves to QD<sub>2</sub> bringing QD<sub>2</sub> back to the even ground state. Crucially, the two electrons that entered the double dot system from the left lead in steps (1) and (3) are absorbed into the right lead as a Cooper pair in step (4).

Gating QD<sub>1</sub> to the 0-1 charge degeneracy point results in Andreev blockade, which is illustrated in Fig. 3(b). The transport cycle proceeds through the same steps, but becomes stuck at step (4) as an inter-dot triplet, that is incompatible with Andreev reflection, is formed on step (3).

<sup>1</sup>We note that for the case with two superconducting leads,  $U_{12}$  induces the quantum state with even parity on both quantum dots to become mixed, which we take into account in our numerics.

### 3 Breakdown of Andreev blockade

Andreev blockade breaks down when single electrons are allowed to tunnel into the superconducting lead as quasiparticles. Quasiparticle excitations become important in two experimentally relevant cases. First, at sufficiently high source-drain bias the quasiparticle states above the superconducting gap become accessible (Fig. 2(c)). Second, superconductors can have low-energy quasiparticles due to nodes in the order parameter, vortices, or disorder. Andreev blockade is also lifted by any spin mixing mechanism, such as due to hyperfine, spin-orbit or electron-phonon interactions [28–30]. Since spin mixing in double dots has been studied previously and is not specific to superconductors, here we focus on quasiparticle transport.

We model a single superconducting lead with a quasiparticle density (a gapless superconductor) using a two-lead model, following Ref. [27]. The first virtual lead describes Cooper pair tunneling, and we model its effect on the adjacent quantum dot using Eq. (1). The second virtual lead describes single particle transport into the superconductor, and is modeled as a normal metal with a variable density of states. The tunneling of single electrons between the quantum dot and the second virtual lead is assumed to be an incoherent process, which we model at the master equation level.

Let us now consider transport in the (normal lead)-(double quantum dot)-(gapless superconducting lead) setup. The subgap density of states (soft gap) is very common in experiments [27]. Naively, we expect that transport can occur either through Andreev reflection or through normal single-particle transport and hence we can find the total current by adding up the two contributions (i.e. superimposing Figs. 2(a) and (b)). Transport calculations (Fig. 4(a)) are largely consistent with this notion, for example the upper right charge degeneracy point is no longer blocked, and the triangles are doubled at each degeneracy point.

However, there is also a qualitatively new feature: transport is allowed in the bottom right corner that was blocked both in Andreev and Pauli cases. The single electron tunneling processes opens a pathway for clearing the inter-dot triplet state as illustrated in Fig. 4(b). The presence of the finite density of states near the chemical potential breaks the blockade by allowing spin-up Andreev bound state to leak out into the lead.

The zero- and finite-temperature charge stability diagrams for the case in which both leads are gapless superconductors are depicted in Figs. 4(c) and (d). The interplay of normal and Andreev transport results in an intermediate charge stability diagram with current at all four charge degeneracy points. At zero temperature, the charge stability diagrams with two gapless superconducting leads Fig. 4(c) and two normal metal leads Fig. 2(a) are clearly distinguishable. At finite temperature the distinction becomes blurred and in general no strong blockade of either kind is observed. The bottom right degeneracy point still shows lower current than the other three. Fig. 4(d) closely matches recent data on double quantum dots with two gapless superconducting leads [27], where this regime has been interpreted as Pauli blockade based on blockade lifting due to spin-orbit interaction observed at finite field.

### 4 Conclusions and outlook

We have proposed a transport phenomenon that occurs in double quantum dots with a superconducting lead. The origin of the proposed Andreev blockade is that a low-lying triplet state suppresses Andreev reflection because electrons from the double dot cannot tunnel into the superconductor as a Cooper pair. The experimental consequence of Andreev blockade is the interruption of transport at two of the four charge degeneracy points (as compared to one of the four for Pauli blockade). Such regime has now been reported experimentally [1].

Quantum dots coupled to superconductors are at the crossroads of several promising research directions such as topological quantum computing, hybrid superconducting quantum bits [31, 32] and quantum simulation. The key experimental technology that enabled the search for Andreev blockade in experiment was to combine the quantum dot setup with a hard gap superconductivity [33, 34].

Proposed topological quantum computing architectures feature single and double quantum dots for Majorana state readout [35–37]. Superconducting double dots are investigated in the context of crossed Andreev reflection which is a key ingredient in recent parafermion proposals [38, 39]. Finally, chains of superconducting quantum dots have been proposed as emulators of the one-dimensional Kitaev model [40–42]. Andreev blockade phenomena may manifest in all of the above situations and can be leveraged to enhance advanced quantum device functionality.

## Acknowledgements

We thank A. Tacla for insightful discussions. DP and SMF acknowledge support from the Charles E. Kaufman foundation, NSF PIRE-1743717. SMF acknowledges NSF DMR-1252962, NSF DMR-1743972, NSF DMR-1906325, ONR and ARO.

## References

- [1] P. Zhang, H. Wu, J. Chen, S. A. Khan, P. Krogstrup, D. Pekker and S. M. Frolov, *Evidence of Andreev blockade in a double quantum dot coupled to a superconductor*, [arXiv:2102.03283](https://arxiv.org/abs/2102.03283).
- [2] A. Imamoğlu, H. Schmidt, G. Woods and M. Deutsch, *Strongly interacting photons in a nonlinear cavity*, *Phys. Rev. Lett.* **79**, 1467 (1997), doi:[10.1103/physrevlett.79.1467](https://doi.org/10.1103/physrevlett.79.1467).
- [3] M. Ciorga, A. S. Sachrajda, P. Hawrylak, C. Gould, P. Zawadzki, S. Jullian, Y. Feng and Z. Wasilewski, *Addition spectrum of a lateral dot from Coulomb and spin-blockade spectroscopy*, *Phys. Rev. B* **61**, R16315 (2000), doi:[10.1103/physrevb.61.r16315](https://doi.org/10.1103/physrevb.61.r16315).
- [4] K. M. Birnbaum, A. Boca, R. Miller, A. D. Boozer, T. E. Northup and H. J. Kimble, *Photon blockade in an optical cavity with one trapped atom*, *Nature* **436**, 87 (2005), doi:[10.1038/nature03804](https://doi.org/10.1038/nature03804).
- [5] J. Koch and F. von Oppen, *Franck-Condon blockade and giant Fano factors in transport through single molecules*, *Phys. Rev. Lett.* **94**, 206804 (2005), doi:[10.1103/physrevlett.94.206804](https://doi.org/10.1103/physrevlett.94.206804).
- [6] R. Leturcq, C. Stampfer, K. Inderbitzin, L. Durrer, C. Hierold, E. Mariani, M. G. Schultz, F. von Oppen and K. Ensslin, *Franck-Condon blockade in suspended carbon nanotube quantum dots*, *Nat. Phys.* **5**, 327 (2009), doi:[10.1038/nphys1234](https://doi.org/10.1038/nphys1234).
- [7] Y.-x. Liu, A. Miranowicz, Y. B. Gao, J. Bajer, C. P. Sun and F. Nori, *Qubit-induced phonon blockade as a signature of quantum behavior in nanomechanical resonators*, *Phys. Rev. A* **82**, 032101 (2010), doi:[10.1103/physreva.82.032101](https://doi.org/10.1103/physreva.82.032101).
- [8] T. A. Fulton and G. J. Dolan, *Observation of single-electron charging effects in small tunnel junctions*, *Phys. Rev. Lett.* **59**, 109 (1987), doi:[10.1103/PhysRevLett.59.109](https://doi.org/10.1103/PhysRevLett.59.109).
- [9] D. V. Averin, A. N. Korotkov and K. K. Likharev, *Theory of single-electron charging of quantum wells and dots*, *Phys. Rev. B* **44**, 6199 (1991), doi:[10.1103/PhysRevB.44.6199](https://doi.org/10.1103/PhysRevB.44.6199).

- [10] C. W. J. Beenakker, *Theory of Coulomb-blockade oscillations in the conductance of a quantum dot*, Phys. Rev. B **44**, 1646 (1991), doi:[10.1103/PhysRevB.44.1646](https://doi.org/10.1103/PhysRevB.44.1646).
- [11] L. J. Geerligs, V. F. Anderegg, J. Romijn and J. E. Mooij, *Single Cooper-pair tunneling in small-capacitance junctions*, Phys. Rev. Lett. **65**, 377 (1990), doi:[10.1103/PhysRevLett.65.377](https://doi.org/10.1103/PhysRevLett.65.377).
- [12] D. B. Haviland, L. S. Kuzmin, P. Delsing and T. Claeson, *Observation of the Coulomb blockade of Cooper pair tunnelling in single Josephson junctions*, Europhys. Lett. **16**, 103 (1991), doi:[10.1209/0295-5075/16/1/018](https://doi.org/10.1209/0295-5075/16/1/018).
- [13] K. Ono, *Current rectification by Pauli exclusion in a weakly coupled double quantum dot system*, Science **297**, 1313 (2002), doi:[10.1126/science.1070958](https://doi.org/10.1126/science.1070958).
- [14] A. C. Johnson, J. R. Petta, C. M. Marcus, M. P. Hanson and A. C. Gossard, *Singlet-triplet spin blockade and charge sensing in a few-electron double quantum dot*, Phys. Rev. B **72**, 165308 (2005), doi:[10.1103/PhysRevB.72.165308](https://doi.org/10.1103/PhysRevB.72.165308).
- [15] R. Hanson, L. P. Kouwenhoven, J. R. Petta, S. Tarucha and L. M. K. Vandersypen, *Spins in few-electron quantum dots*, Rev. Mod. Phys. **79**, 1217 (2007), doi:[10.1103/RevModPhys.79.1217](https://doi.org/10.1103/RevModPhys.79.1217).
- [16] J.-D. Pillet, C. H. L. Quay, P. Morfin, C. Bena, A. Levy Yeyati and P. Joyez, *Andreev bound states in supercurrent-carrying carbon nanotubes revealed*, Nat. Phys. **6**, 965 (2010), doi:[10.1038/nphys1811](https://doi.org/10.1038/nphys1811).
- [17] R. S. Deacon, Y. Tanaka, A. Oiwa, R. Sakano, K. Yoshida, K. Shibata, K. Hirakawa and S. Tarucha, *Tunneling spectroscopy of Andreev energy levels in a quantum dot coupled to a superconductor*, Phys. Rev. Lett. **104**, 076805 (2010), doi:[10.1103/physrevlett.104.076805](https://doi.org/10.1103/physrevlett.104.076805).
- [18] T. Dirks, T. L. Hughes, S. Lal, B. Uchoa, Y.-F. Chen, C. Chialvo, P. M. Goldbart and N. Mason, *Transport through Andreev bound states in a graphene quantum dot*, Nat. Phys. **7**, 386 (2011), doi:[10.1038/nphys1911](https://doi.org/10.1038/nphys1911).
- [19] K. Grove-Rasmussen, G. Steffensen, A. Jellinggaard, M. H. Madsen, R. Žitko, J. Paaske and J. Nygård, *Yu-Shiba-Rusinov screening of spins in double quantum dots*, Nat. Commun. **9**, 2376 (2018), doi:[10.1038/s41467-018-04683-x](https://doi.org/10.1038/s41467-018-04683-x).
- [20] M.-S. Choi, C. Bruder and D. Loss, *Spin-dependent Josephson current through double quantum dots and measurement of entangled electron states*, Phys. Rev. B **62**, 13569 (2000), doi:[10.1103/PhysRevB.62.13569](https://doi.org/10.1103/PhysRevB.62.13569).
- [21] P. Recher, E. V. Sukhorukov and D. Loss, *Andreev tunneling, Coulomb blockade, and resonant transport of nonlocal spin-entangled electrons*, Phys. Rev. B **63**, 165314 (2001), doi:[10.1103/PhysRevB.63.165314](https://doi.org/10.1103/PhysRevB.63.165314).
- [22] J. Eldridge, M. G. Pala, M. Governale and J. König, *Superconducting proximity effect in interacting double-dot systems*, Phys. Rev. B **82**, 184507 (2010), doi:[10.1103/PhysRevB.82.184507](https://doi.org/10.1103/PhysRevB.82.184507).
- [23] Y. Tanaka, N. Kawakami and A. Oguri, *Correlated electron transport through double quantum dots coupled to normal and superconducting leads*, Phys. Rev. B **81**, 075404 (2010), doi:[10.1103/PhysRevB.81.075404](https://doi.org/10.1103/PhysRevB.81.075404).

- [24] C. Padurariu and Yu. V. Nazarov, *Spin blockade qubit in a superconducting junction*, Europhys. Lett. **100**, 57006 (2012), doi:[10.1209/0295-5075/100/57006](https://doi.org/10.1209/0295-5075/100/57006).
- [25] S. Droste, S. Andergassen and J. Splettstoesser, *Josephson current through interacting double quantum dots with spin-orbit coupling*, J. Phys.: Condens. Matter **24**, 415301 (2012), doi:[10.1088/0953-8984/24/41/415301](https://doi.org/10.1088/0953-8984/24/41/415301).
- [26] D. Bouman et al., *Triplet-blockaded Josephson supercurrent in double quantum dots*, Phys. Rev. B **102**, 220505 (2020), doi:[10.1103/PhysRevB.102.220505](https://doi.org/10.1103/PhysRevB.102.220505).
- [27] Z. Su, A. B. Tacla, M. Hocevar, D. Car, S. R. Plissard, E. P. A. M. Bakkers, A. J. Daley, D. Pekker and S. M. Frolov, *Andreev molecules in semiconductor nanowire double quantum dots*, Nat. Commun. **8**, 585 (2017), doi:[10.1038/s41467-017-00665-7](https://doi.org/10.1038/s41467-017-00665-7).
- [28] F. H. L. Koppens, *Control and detection of singlet-triplet mixing in a random nuclear field*, Science **309**, 1346 (2005), doi:[10.1126/science.1113719](https://doi.org/10.1126/science.1113719).
- [29] T. Meunier et al., *Experimental signature of phonon-mediated spin relaxation in a two-electron quantum dot*, Phys. Rev. Lett. **98**, 126601 (2007), doi:[10.1103/physrevlett.98.126601](https://doi.org/10.1103/physrevlett.98.126601).
- [30] A. Pfund, I. Shorubalko, K. Ensslin and R. Leturcq, *Suppression of spin relaxation in an InAs nanowire double quantum dot*, Phys. Rev. Lett. **99**, 036801 (2007), doi:[10.1103/physrevlett.99.036801](https://doi.org/10.1103/physrevlett.99.036801).
- [31] G. de Lange, B. van Heck, A. Bruno, D. J. van Woerkom, A. Geresdi, S. R. Plissard, E. P. A. M. Bakkers, A. R. Akhmerov and L. DiCarlo, *Realization of microwave quantum circuits using hybrid superconducting-semiconducting nanowire Josephson elements*, Phys. Rev. Lett. **115**, 127002 (2015), doi:[10.1103/physrevlett.115.127002](https://doi.org/10.1103/physrevlett.115.127002).
- [32] T. W. Larsen, K. D. Petersson, F. Kuemmeth, T. S. Jespersen, P. Krogstrup, J. Nygård and C. M. Marcus, *Semiconductor-nanowire-based superconducting qubit*, Phys. Rev. Lett. **115**, 127001 (2015), doi:[10.1103/physrevlett.115.127001](https://doi.org/10.1103/physrevlett.115.127001).
- [33] W. Chang, S. M. Albrecht, T. S. Jespersen, F. Kuemmeth, P. Krogstrup, J. Nygård and C. M. Marcus, *Hard gap in epitaxial semiconductor-superconductor nanowires*, Nat. Nanotechnol. **10**, 232 (2015), doi:[10.1038/nnano.2014.306](https://doi.org/10.1038/nnano.2014.306).
- [34] S. Gazibegovic et al., *Epitaxy of advanced nanowire quantum devices*, Nature **548**, 434 (2017), doi:[10.1038/nature23468](https://doi.org/10.1038/nature23468).
- [35] D. Aasen et al., *Milestones toward Majorana-based quantum computing*, Phys. Rev. X **6**, 031016 (2016), doi:[10.1103/physrevx.6.031016](https://doi.org/10.1103/physrevx.6.031016).
- [36] T. Karzig et al., *Scalable designs for quasiparticle-poisoning-protected topological quantum computation with Majorana zero modes*, Phys. Rev. B **95**, 235305 (2017), doi:[10.1103/physrevb.95.235305](https://doi.org/10.1103/physrevb.95.235305).
- [37] S. Plugge, A. Rasmussen, R. Egger and K. Flensberg, *Majorana box qubits*, New J. Phys. **19**, 012001 (2017), doi:[10.1088/1367-2630/aa54e1](https://doi.org/10.1088/1367-2630/aa54e1).
- [38] L. Hofstetter, S. Csonka, J. Nygård and C. Schönenberger, *Cooper pair splitter realized in a two-quantum-dot Y-junction*, Nature **461**, 960 (2009), doi:[10.1038/nature08432](https://doi.org/10.1038/nature08432).
- [39] J. Klinovaja and D. Loss, *Time-reversal invariant parafermions in interacting Rashba nanowires*, Phys. Rev. B **90**, 045118 (2014), doi:[10.1103/physrevb.90.045118](https://doi.org/10.1103/physrevb.90.045118).

- [40] J. D. Sau and S. D. Sarma, *Realizing a robust practical Majorana chain in a quantum-dot-superconductor linear array*, Nat. Commun. **3**, 964 (2012), doi:[10.1038/ncomms1966](https://doi.org/10.1038/ncomms1966).
- [41] I. C. Fulga, A. Haim, A. R. Akhmerov and Y. Oreg, *Adaptive tuning of Majorana fermions in a quantum dot chain*, New J. Phys. **15**, 045020 (2013), doi:[10.1088/1367-2630/15/4/045020](https://doi.org/10.1088/1367-2630/15/4/045020).
- [42] P. Zhang and F. Nori, *Majorana bound states in a disordered quantum dot chain*, New J. Phys. **18**, 043033 (2016), doi:[10.1088/1367-2630/18/4/043033](https://doi.org/10.1088/1367-2630/18/4/043033).